IMPROVING THE ACOUSTIC PERFORMANCE OF EXPANSION CHAMBERS BY USING MICROPERFORATED PANEL ABSORBERS

Alexander Mattioli Pasqual, pasqual@fem.unicamp.br
José Roberto de França Arruda, arruda@fem.unicamp.br
Faculdade de Engenharia Mecânica
Universidade Estadual de Campinas
Rua Mendeleiev, 200
Cidade Universitária "Zeferino Vaz"
13083-970, Campinas, SP, Brazil

Abstract. The purpose of this work is to investigate the effects of the presence of Microperforated Panel Absorbers (MPA) on the sound wave attenuation provided by axisymmetric expansion chambers. The Boundary Element Method (BEM) is used in order to evaluate the Transmission Loss (TL) for a given expansion chamber with different MPA configurations. Plane wave analytical solutions are also presented and compared with BEM results. It is shown that the presence of MPA increases the TL values at certain frequencies and can be used as an alternative to the conventional fibrous absorbing materials. The MPA are located at the ends of the expansion chamber. The impedance of the Microperforated Panel is modeled with Maa's analytical formulation. The MPA can be tuned to increase the TL in the frequency range where the reactive effect decreases.

Keywords: mufflers, microperforated panels, transmission loss, microperforated absorbers, acoustic impedance.

1. INTRODUCTION

Passive mufflers are widely employed to reduce noise in ducts and pipes. Mufflers based on impedance mismatch, called reactive or reflective mufflers, have been most common in the automobile industry. On the other hand, mufflers based on the conversion of acoustic energy into heat by means of porous linings, called dissipative mufflers, are generally used in heat, ventilation and air-conditioning systems (Munjal, 1998).

Expansion chambers are very usual reactive mufflers employed to attenuate the sound radiated by reciprocating machines, like compressors and internal combustion engines. The mufflers are placed in the intake and/or discharge of gases of such machines. Unfortunately, the efficiency of reactive mufflers is enormously reduced at frequencies above the cut-off frequency of the chamber. This can be dealt with by placing fibrous absorbing materials inside the chamber, so that one has a hybrid reactive/dissipative muffler. However, when a clean absorbent system is desirable, it is not possible to add fibrous materials. In this work, the use of Microperforated Panels (MPP) as an alternative to conventional fibrous materials is discussed.

An MPP is a very thin perforated plate in which the diameter of the holes is reduced to submillimeter size. When an MPP is fixed before a rigid surface, so that a cavity is formed between them, one has a Microperforated Panel Absorber (MPA). The behavior of an MPP can be described by its impedance, which was derived by Maa (1998). In this work, the effects of the presence of an MPA inside of an axisymmetric expansion chamber with extended inlet are investigated. The performance parameter used is the Transmission Loss (TL), which is evaluated by the Boundary Element Method (BEM) for different MPP configurations. Plane wave analytical predictions are also presented.

2. EXPANSION CHAMBER WITH EXTENDED INLET AND MPA

Figure 1 illustrates a circular expansion chamber with extended inlet and with an MPP placed near the left wall of the chamber leaving a cavity, thus forming an MPA.
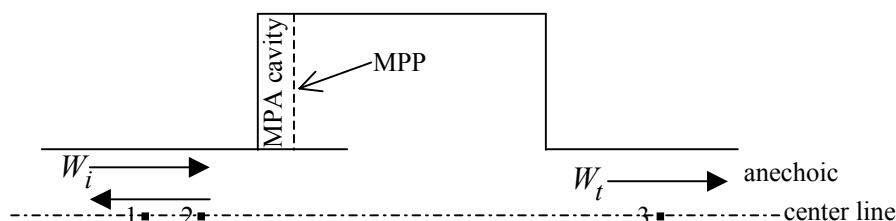
Figure 1. Expansion chamber with extended inlet and MPA.

2.1. Transmission Loss (TL)

The acoustic attenuation performance of an expansion chamber can be described by its Transmission Loss (TL), which is defined as the difference between the sound power level of the incoming wave (W_i) and the sound power level of the wave transmitted (W_t) to an anechoic termination.

According to Wu *et al.* (1998), by selecting two points at the inlet tube and one point at the outlet tube (points 1, 2 and 3, see Fig. 1), the TL can be evaluated for frequencies below the cut-off frequency of the inlet and outlet tubes by

$$TL = 20\log_{10}\left|\frac{p_i}{p_3}\right| + 10\log_{10}\left(\frac{S_i}{S_o}\right) \tag{1}$$

where p_3 is the complex sound pressure amplitude at point 3, S_i and S_o are the cross-sectional areas of the inlet and outlet pipes, respectively, and, provided that $\sin[k(x_2 - x_1)] \neq 0$,

$$p_i = \frac{1}{2j}\frac{\left(p_1 e^{jkx_2} - p_2 e^{jkx_1}\right)}{\sin[k(x_2 - x_1)]} \tag{2}$$

where $j = \sqrt{-1}$, p_1 and p_2 are the complex sound pressure amplitudes at points 1 and 2, k is the wave number, x_1 and x_2 are the longitudinal co-ordinates of the points 1 and 2.

2.2. MPP impedance and MPA absorption

The specific acoustic impedance for a short narrow tube is (Maa, 1998)

$$Z = \rho(r + jx_m) \tag{3}$$

where ρ is the density of the air and

$$r = \frac{32\eta t}{\rho d^2}\left[\left(1 + \frac{k_p^2}{32}\right)^{1/2} + \frac{\sqrt{2}}{32}k_p\frac{d}{t}\right] \tag{4}$$

$$x_m = \omega t\left[1 + \left(1 + \frac{k_p^2}{2}\right)^{-1/2} + 0.85\frac{d}{t}\right] \tag{5}$$

where η is the viscosity of the air, ω is the angular frequency, t is the thickness of the panel, d is the diameter of the holes and

$$k_p = d\sqrt{\frac{\omega\rho}{4\eta}} \tag{6}$$

is the perforate constant.

The impedance of the MPP is defined as

$$Z_{mpp} = \frac{\Delta p}{u} \tag{7}$$

where Δp is the sound pressure jump across the panel and u is the average value of the particle velocity in the panel surface.

By considering the MPP as a lattice of short narrow tubes, the following expression for the impedance of the MPP can be obtained:

$$Z_{mpp} = \frac{Z}{\sigma} \tag{8}$$

where σ is the ratio between the perforated area of the panel and its total area (porosity).

By assuming normal incidence, the sound absorption coefficient, α, of an MPA is (Maa, 1998)

$$\alpha = \frac{4r/(c\sigma)}{[1+r/(c\sigma)]^2 + [x_m/(c\sigma) - \cot(\omega D/c)]^2} \tag{9}$$

where D is the MPA cavity depth.

3. BOUNDARY ELEMENT METHOD

3.1. Axisymmetric formulation

The well-known integral boundary equation for the Helmholtz equation is (Wu, 2000)

$$C(P)p(P) = -\int_S \left[j\rho\omega u_n(Q)\psi(Q,P) + p(Q)\frac{\partial\psi}{\partial n}(Q,P) \right] dS(Q) \tag{10}$$

where P is the collocation point, Q is the integration point, p is the complex sound pressure amplitude, S is the boundary surface, $\vec{n}$ is the normal vector pointing away form the acoustic domain, u_n is the particle velocity in the direction of $\vec{n}$, ψ is the fundamental solution and, for interior problems

$$C(P) = \begin{cases} 1 & , \text{in the domain} \\ 0 & , \text{outside the domain} \\ -\int_S \frac{\partial\psi_L}{\partial n}(Q,P) dS(Q) & , \text{at the boundary} \end{cases} \tag{11}$$

where ψ_L is the fundamental solution of the Laplace equation. The fundamental solutions in a three-dimensional free space are (Wu, 2000)

$$\psi(Q,P) = \frac{e^{-jkR(Q,P)}}{4\pi R(Q,P)} \tag{12}$$

and

$$\psi_L(Q,P) = \frac{1}{4\pi R(Q,P)} \tag{13}$$

where $R(Q,P)$ is the distance between Q and P.

By considering axial symmetry, Equation (10) can be rewritten as

$$C(P)p(P) = -\int_\Gamma j\rho\omega u_n \left(\int_0^{2\pi} \psi\, d\theta \right) r d\Gamma - \int_\Gamma p \left(\int_0^{2\pi} \frac{\partial\psi}{\partial n} d\theta \right) r d\Gamma \tag{14}$$

where $dS = rd\theta d\Gamma$, r is the radial coordinate, θ is the angular coordinate and Γ is the boundary of a two-dimensional domain.

3.2. Multidomain models

An expansion chamber with extended inlet and with an MPP can be modeling by dividing it in three subregions according to the extended inlet length and MPP position, as shown in Fig. 2. Observe that subregion III is the MPA cavity.

The segments AD and FG do not need to be meshed, since they do not belong to the boundary. In order to link the subregions **I** and **II**, the mesh of the segment CD must be equal to the one of the segment EF and one must add

compatibility equations, i.e., pressure and velocity continuity. To properly simulate the MPP, the mesh of the segment KL must be the same as that one of the segment IJ and one must add velocity continuity and pressure jump equations. This last one is given by the impedance of the MPP (Eq. (8)).

The boundary conditions are: unitary normal velocity at AB, impedance equals to ρc at GH (anechoic termination) and zero normal velocity at the walls (rigid walls), where c is the sound speed.
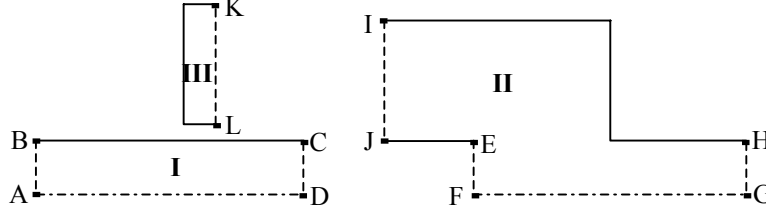
Figure 2. Expansion chamber with extended inlet and MPA divided in three subregions.

In the next section, it will be seen that it is useful to put a rigid ring inside the MPA cavity in order to avoid the propagation of high order modes inside of it. This configuration can be modeled as shown in Fig. 3.
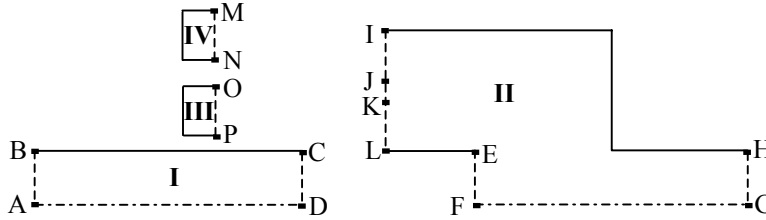
Figure 3. Expansion chamber with extended inlet and MPA divided in four subregions.

To properly simulate the MPP, the meshes of segments KL and IJ must be the same as the ones of segments OP and MN, respectively. The thickness of the ring is equal to the JK length.

4. RESULTS AND DISCUSSION

For the simulations, an extended inlet expansion chamber with an MPP placed inside of it is considered, as shown in Fig. 1. The following dimensions are used: radius of the chamber 72.5mm, radius of the inlet and outlet pipes 18.5mm, total length of the chamber 200mm, length of the outlet pipe 50mm and length of the inlet pipe 50+28mm (28mm is the length of the extension). It is assumed $\rho = 1.2\text{kg/m}^3$, $c = 340\text{m/s}$ and $\eta = 18\text{x}10^{-6}$ Ns/m^2. The boundary is meshed with linear isoparametric elements, whose lengths are smaller than 4mm. The calculations were performed by a BEM software developed by one of the authors. The two MPA configurations shown in Tab. 1 were simulated:

Table 1. MPA configurations.

MPA configuration	D (mm)	t (mm)	d (mm)	σ (%)
# 1	4	0.5	0.4	1.55
# 2	7	0.5	0.7	0.25

Figure 4 shows the absorption coefficients obtained by Eq. (9) for the MPA configurations presented in Tab. 1. These curves are valid only for normal incidence. So, it is not expected to find a good correspondence between these values and the experimental TL at frequencies higher than the cut-off frequency of the chamber, which is approximately 2860Hz for the chamber simulated in this work, corresponding to its first radial mode.
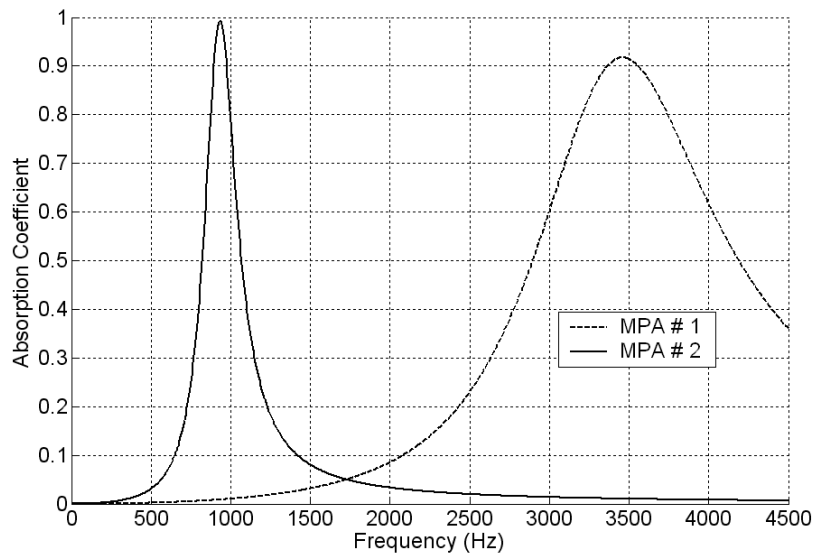
Figure 4. Absorption coefficients for the MPA configurations shown in Tab. 1.

Figure 5 presents the TL curves obtained by the plane wave analytical approximation for the extended inlet expansion chamber without MPA and with the MPA # 2. One can easily verify by observing Figs. 4 and 5 that the MPA dissipative effect, whose peak is around 900Hz, improves significantly the acoustic performance of the chamber at this frequency band. However, such an improvement could be achieved without an MPA, e.g., by using an extended outlet. This could be done since only plane waves propagate at the frequency band in which this MPA works, so that reactive controllers would be efficient too. The vertical dashed line indicates the cut-off frequency of the chamber. So, it is not expected that the results shown in Fig. 5 will be valid for frequencies above this value.

In the results shown in Fig. 5, in order to take into account the radiation impedance, the extended inlet length was increased according to (Munjal, 1987)

$$\Delta L = 0.6a \tag{15}$$

where ΔL is the end correction and a is the radius of the inlet tube.
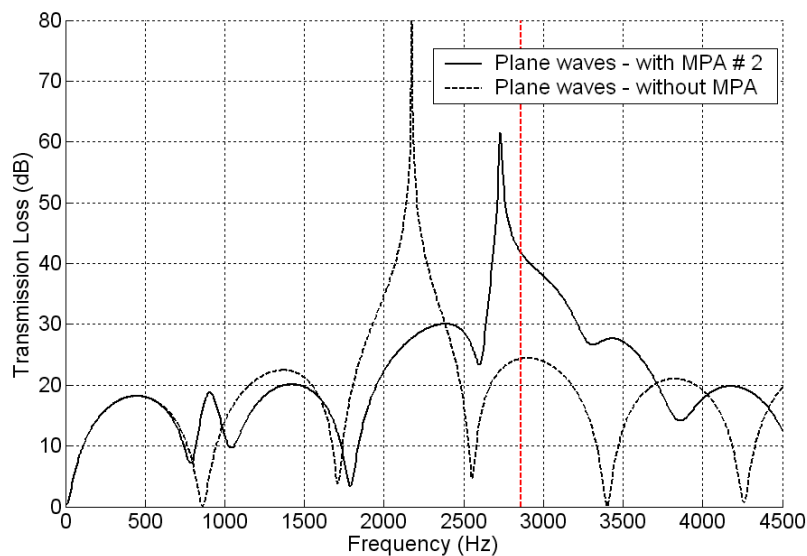
Figure 5. TL curves for an extended inlet expansion chamber without MPA and with MPA # 2 (plane wave solutions).

Figure 6 compares the BEM and plane wave analytical results for the expansion chamber with MPA # 2. One can verify that the analytical solution does not provide good results at frequencies higher than 2.3kHz.
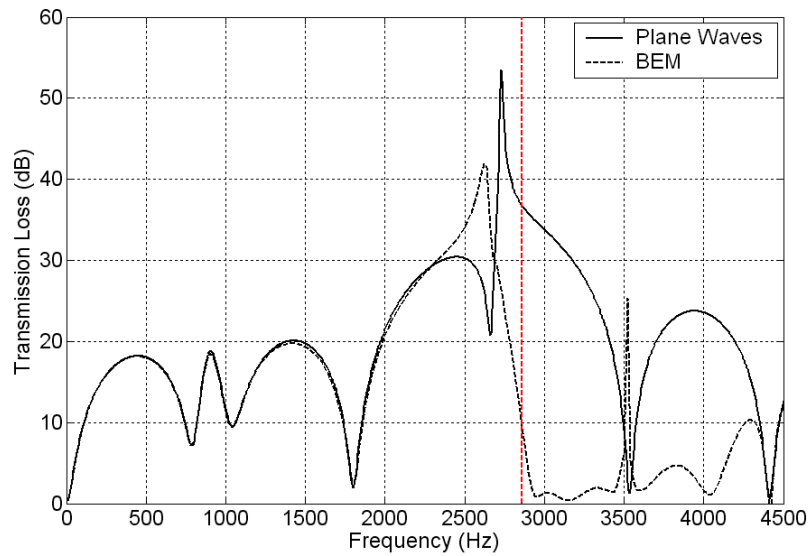
Figure 6. TL curves for an extended inlet expansion chamber with MPA # 2: BEM x Analytical results.

Figure 7 presents the TL curves obtained by the BEM for the extended inlet expansion chamber without MPA and with the MPA # 2.
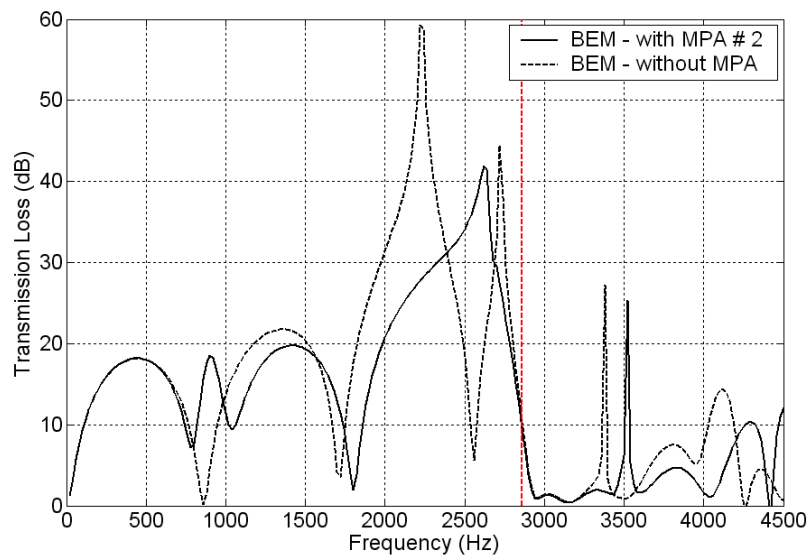
Figure 7. TL curves for an extended inlet expansion chamber without MPA and with MPA # 2 (BEM).

Figure 8 presents the TL curves obtained by the BEM for the extended inlet expansion chamber without MPA and with the MPA # 1. It is shown that the presence of such an MPA does not change appreciably the TL curve. By comparing Figs. 4 and 8, it is not possible to establish a relationship between the TL curve and the MPA dissipative effect, whose peak is around 3500Hz. This occurs since the normal incidence assumption (adopted to plot Fig. 4) is no longer valid for frequencies greater than 2860Hz approximately, which corresponds to the first radial mode of the chamber. This can be dealt with by placing a rigid ring inside the MPA cavity to avoid high order modes propagation in the cavity (see Fig. 3). Figure 9 shows the results obtained by using a 2mm thick ring with radius equals to 45.5mm.
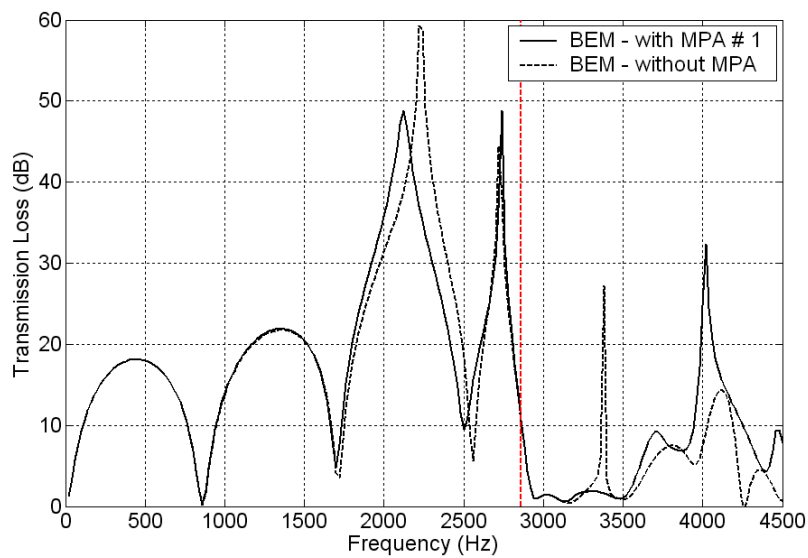
Figure 8. TL curves for an extended inlet expansion chamber without MPA and with MPA # 1 (BEM).
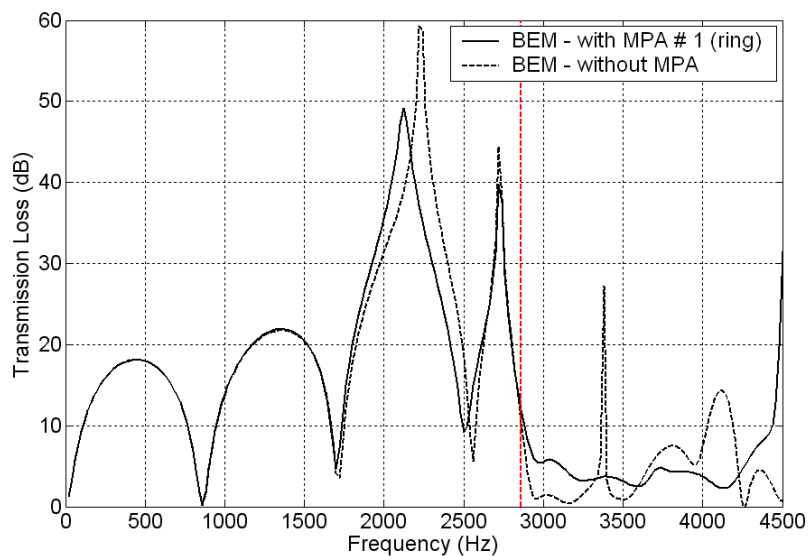
Figure 9. TL curves for an extended inlet expansion chamber without MPA and with MPA # 1 (BEM).

By comparing Figs. 8 and 9, it can be verified the improvement on the TL in the frequency band 3000-3500Hz. The absorption peak of the MPA # 1 occurs near 3500Hz. So, it is suggested that the presence of a ring inside of the MPA cavity permits to use the α curve obtained analytically to estimate the behavior of the TL curve. However, the TL peak at 4000Hz shown in Fig. 8 disappears when the MPA cavity has an inner ring.

The TL can be improved by adding an extended outlet with its own MPA to the chamber. Figure 10 compares the solid TL curve of Fig. 9 with the results obtained by the BEM for the chamber with extended inlet and outlet. The length of the extended outlet and its MPA parameters are the same as that ones of the inlet.
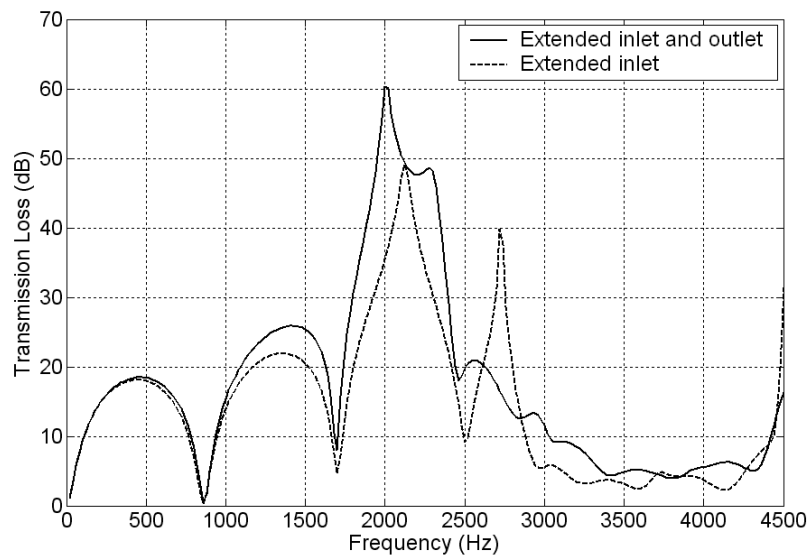
Figure 10. TL curves for an extended inlet/outlet expansion chamber with MPA # 1 (BEM).

5. CONCLUSIONS

In this work, it is shown that MPAs can improve the TL of extended inlet/outlet mufflers at frequencies above the cut-off frequency of the chamber, so that they can be used as an alternative to fibrous absorbing materials. It is also show that the effect of the MPA on the acoustic behavior of the muffler can be qualitatively estimated by evaluating its absorption coefficient for normal incidence. Finally, the MPA can be tuned to increase the TL in the frequency range where the reactive effect decreases.

6. ACKNOWLEDGEMENTS

The authors would like to thank CAPES for the financial support of this work.

7. REFERENCES

Maa, Dah-You, 1998, "Potential of Microperforated Panel Absorber", Journal of Acoustical Society of America, Vol. 104, No. 5, pp. 2861-2866.
Munjal, M. L., 1987, "Acoustics of Ducts and Mufflers – with Application to Exhaust and Ventilation System Design", Ed. John Wiley & Sons, New York.
Munjal, M. L., 1998, "Analysis and Design of Mufflers – An Overview of Research at the Indian Institute of Science", Journal of Sound and Vibration, Vol. 211, No.3, pp. 425-433.
Wu, T. W., 2000, "Boundary Element Acoustics: Fundamentals and Computer Codes", Ed. WIT Press.
Wu, T. W., Zhang, P. and Cheng, C. Y. R., 1998, "Boundary Element Analysis of Mufflers with an Improved Method for Deriving the Four-Pole Parameters", Journal of Sound and Vibration, Vol. 217, No. 4, pp. 767-779.

8. RESPONSIBILITY NOTICE

The authors are the only responsible for the printed material included in this paper.